Size of the freeze-out source in high energy heavy ion collisions*

SHAN Lian-Qiang(单连强)[1] WU Feng-Juan(吴凤娟)[1] GUAN Hui-Jun(关慧君)[2]
ZHANG Jing-Bo(张景波)[1] TANG Gui-Xin(唐圭新)[1] HUO Lei(霍雷)[1;1)]

1 (Department of Physics, Haerbin Institute of Technology, Haerbin 150001, China)
2 (College of Natural Science, Jiamusi University, Jiamusi 154007, China)

Abstract Based on a hydro-inspired azimuthally symmetric emission function, we analyze the HBT radius $R_{\rm s}$ and the single-particle transverse momentum spectra in Au+Au collisions measured by the STAR Collaboration at $\sqrt{s_{\rm NN}} = 200$ GeV. The results show that consistent assumptions about transverse density (and/or flow profile) in the calculation of the HBT radius $R_{\rm s}$ and single-particle spectral analyses play an important role for understanding the size of the freeze-out source.

Key words source size, two-pion interferometry, single-particle spectra

PACS 25.75.-q, 25.75.Gz

1 Introduction

In high energy heavy ion collisions, two-pion interferometry (HBT) is a useful tool to obtain space-time and dynamical information about the source[1, 2]. The HBT radius parameters obtained from fitting the two-pion correlation function measure the homogeneity regions of the source from which particles are emitted with a given momentum[3]. The transverse mass $M_{\rm T}$ dependence of the HBT radius $R_{\rm s}$ is often used to extract the geometric size of the freeze-out source[4, 5]. In theory, the HBT radii can be directly calculated from the emission function[6, 7]. Generally, for an expanding source, $R_{\rm s}$ reflects an interplay between the source size, temperature and velocity gradients. Usually, the temperature and the transverse flow parameter in the expression of $R_{\rm s}$ are obtained by single-particle spectra.

In the calculation of the HBT radius $R_{\rm s}$ from the emission function, a Gaussian transverse density is often assumed, and the transverse flow is either a linear velocity profile or a linear rapidity profile with radial position[6, 7]. However, in single-particle spectral analyses, it is often assumed that the transverse density distribution is uniform inside a surface radius $R_{\rm b}$ (box profile) and the flow velocity varies with radial position as a power law[8, 9]. Sometimes, the transverse Gaussian radius and the velocity at Gaussian radius in the $R_{\rm s}$ formula are considered to be some kind of equivalent geometric surface radius and surface velocity[5]. In this paper, we analyze the transverse momentum spectra and HBT radius $R_{\rm s}$ using the same hydro-inspired azimuthally symmetric emission function. We discuss the effects of inconsistent assumptions about transverse density (and/or flow profile) in the calculation of the HBT radius $R_{\rm s}$ and single-particle spectral analyses on the size of the freeze-out source.

This paper is organized as follows. Sec. 2 briefly introduces the emission function and discusses the general expression for the HBT radius $R_{\rm s}$ and the transverse momentum spectra. An approximate expression of $M_{\rm T}$ dependence of $R_{\rm s}$ based on the box transverse density and linear flow rapidity is given. In Sec. 3, we perform simultaneous fits to $\pi^{\pm}$, $\rm K^{\pm}$, p, $\overline{\rm p}$ spectra and analyze the HBT radius $R_{\rm s}$ for charged pion in Au+Au collisions at RHIC energy. Finally, conclusions are drawn in Sec. 4.

Received 18 August 2008

* Supported by Science Foundation of Harbin Institute of Technology (HIT 2002.47; 2003.33)

1) E-mail: lhuo@hit.edu.cn

2 Emission function and $M_{\rm T}$ dependence of the HBT radius $R_{\rm s}$

The standard hydrodynamic model can provide an excellent quantitative description the soft $p_{\rm T}$ spectra and elliptic flow but it is invalid for describing pion HBT radii[10]. However, some hydro-inspired parameterizations of the emission function provide a convenient way to interpret the data. We consider the extensively used azimuthally symmetric emission function[7]

$$S(x,\boldsymbol{K}) \propto M_{\rm T}\cosh(\eta-Y){\rm e}^{-K\cdot u/T} f(r)\delta(\tau-\tau_0)\,. \quad (1)$$

The space-time rapidity is labeled as $\eta = \frac{1}{2}\ln[(t+z)/(t-z)]$, and $\tau=\sqrt{t^2-z^2}$ is the longitudinal proper time. $\boldsymbol{K}=\frac{1}{2}(\boldsymbol{p}_1+\boldsymbol{p}_2)$ is the average momentum of the pair. As an approximation, K is often put on shell $K^0\approx\sqrt{m^2+\boldsymbol{K}^2}$. The Boltzmann factor $\exp(-K\cdot u/T)$ arises from the assumption of local thermal equilibrium (temperature T) within a source element moving with four velocity $u(x)$. It is often assumed that there is a boost invariant longitudinal expansion. With the help of the transverse flow rapidity $\rho(r)=\tanh^{-1}v(r)$ and the pair rapidity Y, the four velocity $u(x)$ and the four momentum $\boldsymbol{K}$ are expressed as[7]

$$\begin{aligned} u_\mu(x) &= \big(\cosh\eta\cosh\rho(r), \sinh\rho(r)\frac{x}{r}, \\ &\quad \sinh\rho(r)\frac{y}{r}, \sinh\eta\cosh\rho(r)\big), \quad (2)\\ K_\mu &= \big(M_{\rm T}\cosh Y, K_{\rm T}, 0, M_{\rm T}\sinh Y\big), \end{aligned}$$

where $K_{\rm T}$ is the transverse component of $\boldsymbol{K}$, and $M_{\rm T}=\sqrt{m^2+K_{\rm T}^2}$ is the transverse mass of the pair.

In two-pion interferometry analyses, the relative momentum $\boldsymbol{q}=\boldsymbol{p}_1-\boldsymbol{p}_2$ is decomposed according to the "out-side-long" coordinate system[11]: the longitudinal direction is parallel to the beam direction, the outward direction is parallel to the transverse component $K_{\rm T}$, and the sideward direction is perpendicular to the longitudinal and outward directions. The two-pion correlation function is usually expressed in the longitudinal comoving system (LCMS) frame defined by the vanishing z-component of the pair momentum. Usually, the correlation function can be expressed as[5]

$$C(q,\boldsymbol{K}) = 1+\lambda{\rm e}^{-q_{\rm o}^2R_{\rm o}^2(\boldsymbol{K})-q_{\rm s}^2R_{\rm s}^2(\boldsymbol{K})-q_{\rm l}^2R_{\rm l}^2(\boldsymbol{K})-2q_{\rm o}q_{\rm s}R_{\rm os}^2(\boldsymbol{K})}, \quad (3)$$

where λ is the coherence parameter. $R_{\rm o}$, $R_{\rm s}$, $R_{\rm l}$, and $R_{\rm os}$ are the so-called HBT radii. For central collision or azimuthally integrated analysis, $R_{\rm os}=0$ for the $q_{\rm s}$ symmetry.

The main aim of HBT analysis is to extract as much information as possible about the emission function $S(x,\boldsymbol{K})$, which characterizes the particle emitting source created in the collisions. It has been pointed at that the HBT radii are related to space-time variance as[1, 6, 12]:

$$\begin{aligned} R_{\rm s}^2(\boldsymbol{K}) &= \langle y^2\rangle,\\ R_{\rm o}^2(\boldsymbol{K}) &= \langle(x-v_{\rm o}t)^2\rangle-\langle x-v_{\rm o}t\rangle^2, \quad (4)\\ R_{\rm l}^2(\boldsymbol{K}) &= \langle(z-v_{\rm l}t)^2\rangle-\langle z-v_{\rm l}t\rangle^2, \end{aligned}$$

where $v_{\rm o}$ and $v_{\rm l}$ are the transverse and longitudinal velocities of the pair, respectively. The average notation is defined as

$$\langle\xi\rangle = \frac{\int{\rm d}^4x\,\xi\,S(x,\boldsymbol{K})}{\int{\rm d}^4x\,S(x,\boldsymbol{K})}\,. \quad (5)$$

The HBT radius $R_{\rm s}$ is independent of the time parameter, and it probes the spatial extent of the source. Substituting Eq. (1) into Eq. (4), one can get the following expression at midrapidity:

$$R_{\rm s}^2(M_{\rm T}) = \frac{\int_0^{+\infty}{\rm d}r f(r)\,\frac{r^3}{\alpha}\,I_1(\alpha)\,K_1(\beta)}{\int_0^{+\infty}{\rm d}r f(r)\,r\,I_0(\alpha)\,K_1(\beta)}\,, \quad (6)$$

where I_0, I_1 and K_1 are modified Bessel functions. $\alpha\equiv K_{\rm T}\sinh\rho(r)/T$ and $\beta\equiv M_{\rm T}\cosh\rho(r)/T$. In practice, $f(r)$ in Eq. (6) is often assumed with Gaussian shape $f(r)\propto\exp(-r^2/2R_{\rm g})$. The transverse flow usually has two profiles: the linear flow velocity $v(r)=v_{\rm g}r/R_{\rm g}$[6] and the linear flow rapidity $\rho(r)=\rho_{\rm g}r/R_{\rm g}$[7]. The $M_{\rm T}$ dependence of the HBT radius $R_{\rm s}$ can be approximately expressed as[6, 7]

$$R_{\rm s}(M_{\rm T}) = \frac{R_{\rm g}}{\sqrt{1+v_{\rm g}^2\Big(\frac{M_{\rm T}}{T}\Big)}}\,, \quad (7)$$

$$R_{\rm s}(M_{\rm T}) = \frac{R_{\rm g}}{\sqrt{1+\rho_{\rm g}^2\Big(\frac{1}{2}+\frac{M_{\rm T}}{T}\Big)}}\,. \quad (8)$$

Eq. (7) and Eq. (8) establish contacts between the experimentally observable $R_{\rm s}$ and the freeze-out configurations of the source. Both equations are frequently used to fit the $M_{\rm T}$ dependence of $R_{\rm s}$ to extract the source radius $R_{\rm g}$[4, 5, 13, 14]. The temperature T, and the flow parameter $\rho_{\rm g}$ or $v_{\rm g}$ are usually obtained from simultaneously fitting the transverse momentum spectra of $\pi^{\pm}$, $\rm K^{\pm}$, p, $\overline{\rm p}$ by the following

equation[15]

$$\frac{\mathrm{d}N}{m_{\mathrm{T}}\mathrm{d}m_{\mathrm{T}}} \propto \int \mathrm{d}^4 x S(x,p) \propto \int_0^{+\infty} r\mathrm{d}r f(r) m_{\mathrm{T}} I_0\left(\frac{p_{\mathrm{T}}\sinh\rho}{T}\right) K_1\left(\frac{m_{\mathrm{T}}\cosh\rho}{T}\right). \quad (9)$$

In Eq. (9), the density $f(r)$ is often assumed to be a box profile with surface radius R_{b} and the flow velocity field is usually taken as the power law form $v(r) = v_{\mathrm{b}}(r/R_{\mathrm{b}})^n$. It is known that the values of temperature and flow parameter are model-dependent in single-particle spectral analyses[16, 17]. Therefore, the inconsistent assumptions about the transverse density and flow profile in Eq. (8) (Eq. (7)) and Eq. (9) may induce some ambiguity. Moreover, the value of ρ_{g} (flow rapidity at Gaussian radius) used in Eq. (8) is sometimes replaced by the surface flow rapidity ρ_{b} obtained from single-particle spectral analyses, and the obtained R_{g} is considered to be the geometric surface radius for a Gaussian transverse density profile[5]. To a certain extent, these inconsistencies may induce deviations when one extracts the geometric size of the freeze-out source.

We adopt the transverse box density distribution for extracting the surface radius of the source. Similar to Eq. (8), the linear flow rapidity $\rho(r) = \rho_{\mathrm{b}} r/R_{\mathrm{b}}$ is assumed. Therefore, Eq. (6) can be expressed as:

$$R_{\mathrm{s}}^2(M_{\mathrm{T}}) = \frac{\int_0^{R_{\mathrm{b}}} \mathrm{d}r \frac{r^3}{\alpha} K_1(\beta) I_1(\alpha)}{\int_0^{R_{\mathrm{b}}} \mathrm{d}r\, r\, K_1(\beta) I_0(\alpha)}. \quad (10)$$

In the case of $\rho < 1$, we have the following approximation:

$$\alpha = \frac{K_{\mathrm{T}}}{T}\sinh(\rho) \approx \frac{K_{\mathrm{T}}}{T}\rho,$$
$$\beta^{-\frac{1}{2}} = \left(\frac{M_{\mathrm{T}}}{T}\cosh(\rho)\right)^{-\frac{1}{2}} \approx \sqrt{\frac{T}{M_{\mathrm{T}}}}\left(1-\frac{1}{4}\rho^2\right). \quad (11)$$

The modified Bessel functions can be expanded as

$$I_\upsilon(\alpha) = \sum_{k=0}^{+\infty} \frac{1}{k!\Gamma(k+\upsilon+1)}\left(\frac{\alpha}{2}\right)^{\upsilon+2k},$$
$$K_1(\beta) \approx \sqrt{\frac{\pi T}{2M_{\mathrm{T}}}}\left(1-\frac{1}{4}\rho^2\right)\mathrm{e}^{-\frac{M_{\mathrm{T}}}{T}}\mathrm{e}^{-\frac{M_{\mathrm{T}}}{2T}\rho^2}. \quad (12)$$

With the above approximations, R_{s}^2 can be expressed as:

$$R_{\mathrm{s}}^2 \approx \frac{T}{K_{\mathrm{T}}}\left(\frac{R_{\mathrm{b}}}{\rho_{\mathrm{b}}}\right)^2 \times \frac{BG_1 + \sum_{k=1}^{+\infty}\left[\frac{B^{2k+1}}{k!(k+1)!} - \frac{B^{2k-1}}{4(k-1)!k!}\right]G_{k+1}}{G_0 + \sum_{k=1}^{+\infty}\left[\frac{B^{2k}}{k!k!} - \frac{B^{2k-2}}{4(k-1)!(k-1)!}\right]G_k}, \quad (13)$$

where $B \equiv K_{\mathrm{T}}/(2T)$ and G_k are a series of integrations

$$G_k = \int_0^{\rho_{\mathrm{b}}} \rho^{2k+1}\mathrm{e}^{-A\rho^2}\,\mathrm{d}\rho = \frac{k!}{2A^{k+1}}\left(1-\mathrm{e}^{-A\rho_{\mathrm{b}}^2}\sum_{i=0}^{k}\frac{A^{k-i}}{(k-i)!}\rho_{\mathrm{b}}^{2(k-i)}\right), \quad (14)$$

where $A \equiv M_{\mathrm{T}}/(2T)$. The m_{T} dependence of R_{s} calculated from Eq. (13) is shown in Fig. 1 with solid lines. In the calculation, we take the freeze-out temperature $T = 100$ MeV and surface radius $R_{\mathrm{b}} = 10$ fm. The surface flow rapidity ρ_{b} is taken as 0.3, 0.6, and 1.0, respectively. We only expand k to the third-order term and the higher-order terms are neglected. The dashed lines give the numerical results from Eq. (10).

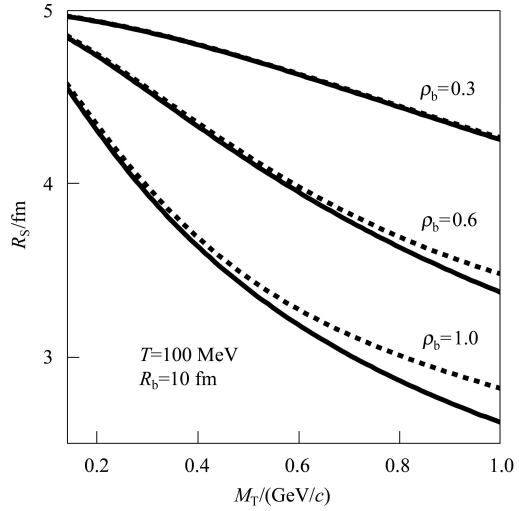

Fig. 1. M_{T} dependence of the HBT radius R_{s} for the emission function Eq. (1). The dashed lines are numerically calculated from Eq. (10), and the solid lines from Eq. (13).

The results show that Eq. (13) gives a good approximation especially at lower flow rapidity ρ_{g} or lower transverse momentum M_{T}. In fact, when $\rho_{\mathrm{b}} = 0.3$, one can get good approximate results even if k is expanded to the first order in Eq. (13). At RHIC energy, ρ_{b} is around the range 0.7—1.0, and m_{T} is usually below 0.8 GeV/c in HBT analyses. It has been pointed out that the decrease of R_{s} with m_{T} indicates the existence of transverse flow[6].

3 Data analysis

The STAR Collaboration has measured single-particle spectra of $\pi^{\pm}$, $K^{\pm}$, p, $\overline{p}$ and two-pion correlation functions in Au+Au collisions at $\sqrt{s_{NN}}=200$ GeV[5, 8]. They use Eq. (9) to simultaneously fit the spectra of $\pi^{\pm}$, $K^{\pm}$, p, $\overline{p}$ for six centrality bins with box transverse density and power law velocity field $v(r)=v_b(r/R_b)^n$. The six centrality bins correspond to (0—5)%, (5—10)%, (10—20)%, (20—30)%, (30—50)%, and (50—80)% of the total hadronic cross section. The results of temperature T and the surface flow rapidity $\rho_b=\tanh^{-1}v_b$ as a function of the number of participants N_{part} are shown in Fig. 2 with open circles. The values of N_{part} are calculated from the Glauber model. We use Eq. (9) to simultaneously fit the spectra of $\pi^{\pm}$, $K^{\pm}$, p, $\overline{p}$ with box density distribution and linear flow rapidity $\rho(r)=\rho_b r/R_b$. The fitted parameters T and ρ_b as a function of N_{part} are shown in Fig. 2 with solid circles (The last two centrality bins are obtained by summing up the (30—40)%, (40—50)% and (50—60)%, (60—70)%, (70—80)% centralities used in Ref. [8], respectively.)

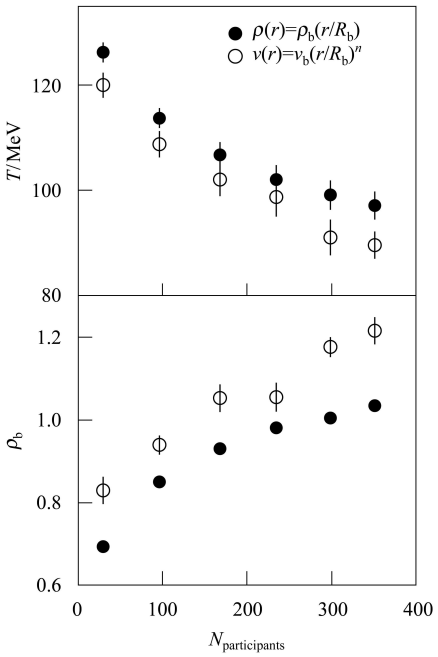

Fig. 2. Freeze-out temperature T, surface flow rapidity as a function of N_{part}. The errors do not include the systematic uncertainties. (open circles are taken from Ref. [5]).

As shown in Fig. 2, the temperature T decreases with centrality and the surface flow rapidity increases with centrality in both analyses. The linear flow rapidity gives a higher temperature and lower surface flow rapidity. In fact, different density distributions can also affect their values[17]. This implies that the values of temperature and flow parameter extracted from single-particle spectra are model-dependent.

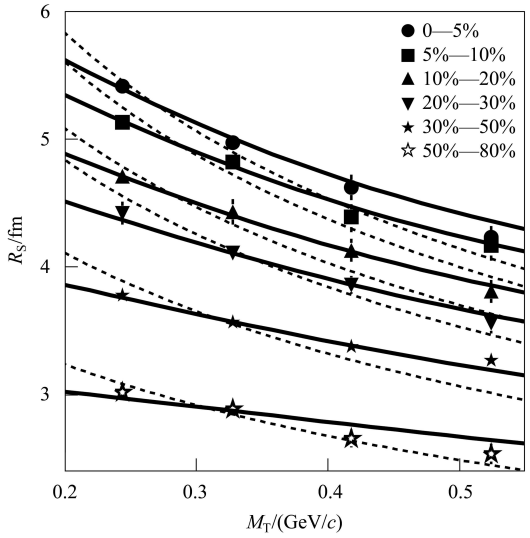

Fig. 3. M_T dependence of the pion HBT radius R_s measured by the STAR Collaboration in Au+Au collisions at $\sqrt{s_{NN}}=200$ GeV for six centrality bins. The solid lines show the fits of Eq. (13), and the dashed lines show the fits of Eq. (8).

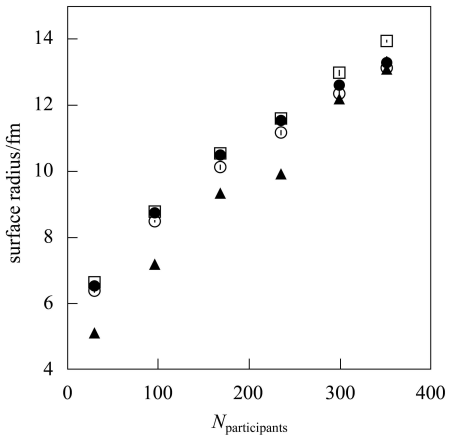

Fig. 4. The extracted surface radii of the freeze-out source as a function of N_{part}. The solid circles and the triangles are taken from Ref. [5]. The open circles and open squares are extracted from fitting R_s to Eq. (13) and Eq. (6) (power law transverse flow profile). Only the fitting error is presented.

In order to extract the transverse surface radius, Ref. [5] has fitted the M_T dependence of the HBT radius R_s to Eq. (8), where the T and ρ_g are given by single-particle spectral analyses with box density and power law flow velocity (open circles in Fig. 2). The fitted curves are shown in Fig. 3 with dashed lines and the obtained equivalent surface radii are shown in Fig. 4 with triangles. The quality of the fits is not

good[5]. It has been indicated that Eq. (8) is based on the Gaussian transverse density and linear flow rapidity, but the values of the open circles given in Fig. 2 are based on the box density and power law flow velocity profile. So, we use Eq. (13) to fit the $M_{\rm T}$ dependence of the HBT radius $R_{\rm s}$ with T and $\rho_{\rm b}$, given by solid circles in Fig. 2. The fitted curves are shown in Fig. 3 with solid lines and the fitted results of surface radii are shown in Fig. 4 with open circles. It can be seen from Fig. 3 that a better agreement between the solid lines and the data is obtained.

Ref. [5] also used a blast-wave model[18] to simultaneously fit the transverse momentum spectra, elliptic flow and HBT radii $R_{\rm s}$, $R_{\rm o}$, $R_{\rm l}$. The parameterization of the blast-wave model is similar to Eq. (1) with box transverse density and linear flow rapidity. The fitting process involves multi-dimensional numerical integration as in Eq. (9) and Eq. (4)[18]. The obtained surface radii are shown in Fig. 4 with solid circles. From Fig. 4, we can see that our results (open circles) are consistent with the simultaneous blast-wave fit. Generally, once some kind of transverse density and transverse flow distribution are adopted in the calculation of $R_{\rm s}$ (Eq. (6)), we should make the same assumptions in single-particle analyses (Eq. (9)) to provide the values of corresponding temperature and flow parameters. If we want to extract the transverse surface radius of the source, it is more direct to assume box density distribution in the emission function. The equivalent surface radius from Eq. (8) is just an approximation. For another example, if we use the box density and the power law velocity profile in Eq. (6), then the values of temperature and flow parameter can be provided by the open circles in Fig. 3. Fitting the $M_{\rm T}$ dependence of $R_{\rm s}$ to Eq. (6), the obtained surface radii are shown in Fig. 4 with open squares. It can be seen that the values of the open squares are also consistent with those of the simultaneous blast-wave fit. Of course, Gaussian density distribution can be used in Eq. (6) (i.e. Eq. (7) or Eq. (8)): then we should use the same assumption in transverse momentum spectral analyses. Which assumption about transverse density distribution (and/or flow profile) is more reasonable may depend on the quality of the fitting. In this paper, we emphasize that the consistency of the assumptions about transverse density (and/or flow profile) in the calculation of the HBT radius $R_{\rm s}$ and transverse momentum spectra is important in extracting the size of the source.

4 Conclusion

With an azimuthally symmetric emission function, we discuss the general expression for the transverse mass spectra and the HBT radius $R_{\rm s}$. Based on the transverse momentum spectral formula and an approximate analytical expression for $M_{\rm T}$ dependence of HBT radius $R_{\rm s}$ with box transverse density and linear flow rapidity, we investigate the transverse momentum spectra of $\pi^{\pm}$, $\rm K^{\pm}$, p, $\overline{\rm p}$ and $M_{\rm T}$ dependence of the pion HBT radius $R_{\rm s}$ measured by the STAR Collaboration in Au+Au collisions at $\sqrt{s_{\rm NN}}$ = 200 GeV. To extract the size of the freeze-out source, it should be reasonable to use the same assumptions about transverse density (and/or flow profile) in the calculation of the HBT radius $R_{\rm s}$ and single-particle spectra.

References

1 Wiedemann U A, Heinz U. Phys. Rep., 1999, **319**: 145—230
2 Lisa M A, Pratt S, Soltz R et al. Ann. Rev. Nucl. Part. Sci., 2005, **55**: 357—402
3 Makhlin A N, Sinyukov Y M. Z. Phys. C, 1988, **39**: 69—73
4 Adcox K et al. (PHENIX Collaboration). Phys. Rev. Lett., 2002, **88**: 192302
5 Adams J et al. (STAR Collaboration). Phys. Rev. C, 2005, **71**: 044906
6 Chapman S, Scotto P, Heinz U. Phys. Rev. Lett., 1995, **74**: 4400—4403
7 Wiedemann U A, Scotto P, Heinz U. Phys. Rev. C, 1996, **53**: 918—931
8 Adams J et al. (STAR Collaboration). Phys. Rev. Lett., 2004, **92**: 112301
9 Adcox K et al. (PHENIX Collaboration). Phys. Rev. C, 2004, **69**: 024904
10 Heinz U, Kolb P. Nucl. Phys. A, 2002, **702**: 269c—280c
11 Bertsch G, Gong M, Tohyama M. Phys. Rev. C, 1988, **37**: 1896—1900
12 Frodermann E, Heinz U, Lisa M A. Phys. Rev. C, 2006, **73**: 044908
13 Adamova D et al. (CERES Collaboration). Nucl. Phys. A, 2003, **714**: 124—144
14 Antinori F et al. (NA57 Collaboration). J. Phys. G, 2007, **34**: 403—429
15 Schnedermann E, Sollfrank J, Heinz U. Phys. Rev. C, 1993, **48**: 2462—2475
16 Esumi S, Chapman S, Hecke H et al. Phys. Rev. C, 1997, **55**: 2163—2166(R)
17 Aggarwal M M et al. (WA98 Collaboration). Phys. Rev. Lett., 1999, **83**: 926—930
18 Retiere F, Lisa M A. Phys. Rev. C, 2004, **70**: 044907